Cell Reports

Article

Tandem bispecific antibody prevents pathogenic $SHIV_{SF162P3CN}$ infection and disease progression

Graphical abstract

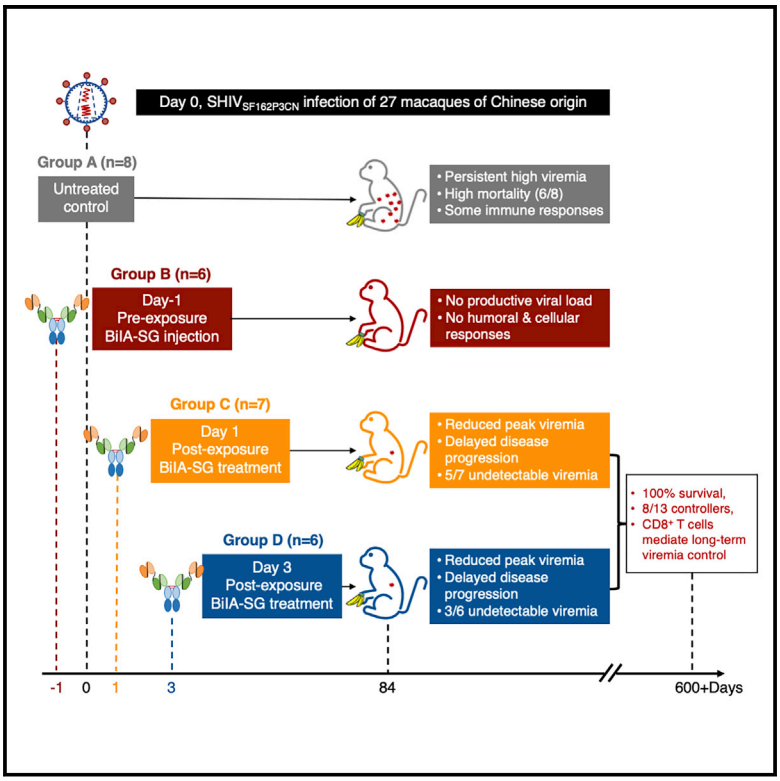

Highlights

- Intravenous $SHIV_{SF162P3CN}$ challenge results in high mortality in Chinese macaques
- Pre-exposure BiIA-SG injection confers protection against $SHIV_{SF162P3CN}$ infection
- Post-exposure BiIA-SG converts pathogenic infection into long-term viremia control
- BiIA-SG therapy-induced $CD8^+$ T cells confer viral suppression in controller animals

Authors

Mengyue Niu, Yik Chun Wong, Hui Wang, ..., Haoji Zhang, Linqi Zhang, Zhiwei Chen

Correspondence

zchenai@hku.hk

In brief

Niu et al. describe a bi-specific broadly neutralizing antibody BiIA-SG in the $SHIV_{SF162P3CN}$/Chinese monkey model. Pre-exposure BiIA-SG injection prevents viral infection. Post-exposure injection achieves undetectable viremia in most animals and delays disease progression for over 2 years. These findings warrant the clinical development of BiIA-SG for HIV-1 prevention and immunotherapy.

Niu et al., 2021, Cell Reports *36*, 109611
August 24, 2021
https://doi.org/10.1016/j.celrep.2021.109611

CellPress

Cell Reports

CellPress
OPEN ACCESS

Article

Tandem bispecific antibody prevents pathogenic $SHIV_{SF162P3CN}$ infection and disease progression

Mengyue Niu,[1,6] Yik Chun Wong,[1,6] Hui Wang,[2,6] Xin Li,[1,3,6] Chun Yin Chan,[1] Qi Zhang,[4] Lijun Ling,[1] Lin Cheng,[2] Ruoke Wang,[4] Yanhua Du,[1] Lok Yan Yim,[1] Xia Jin,[5] Haoji Zhang,[3] Linqi Zhang,[4] and Zhiwei Chen[1,2,7,*]

[1]AIDS Institute and Department of Microbiology, State Key Laboratory of Emerging Infectious Diseases, Li Ka Shing Faculty of Medicine, The University of Hong Kong, Hong Kong SAR, People's Republic of China

[2]HKU-AIDS Institute Shenzhen Research Laboratory and AIDS Clinical Research Laboratory, Guangdong Key Laboratory of Emerging Infectious Diseases, Shenzhen Key Laboratory of Infection and Immunity, Shenzhen Third People's Hospital, Shenzhen, People's Republic of China

[3]Department of Veterinary Medicine, Foshan University, Foshan, People's Repubic of China

[4]Comprehensive AIDS Research Center and Collaborative Innovation Center for Diagnosis and Treatment of Infectious Diseases, School of Medicine, Tsinghua University, Beijing, People's Republic of China

[5]Translational Medical Research Institute, Shanghai Public Health Clinical Center, Fudan University, Shanghai, People's Republic of China

[6]These authors contributed equally

[7]Lead contact

*Correspondence: zchenai@hku.hk

https://doi.org/10.1016/j.celrep.2021.109611

SUMMARY

Although progress has been made on constructing potent bi-specific broadly neutralizing antibody (bi-bNAb), few bi-bNAbs have been evaluated against HIV-1/AIDS in non-human primates (NHPs). Here, we report the efficacy of a tandem bi-bNAb, namely BiIA-SG, in Chinese-origin rhesus macaques (CRM) against the CRM-adapted R5-tropic pathogenic $SHIV_{SF162P3CN}$ challenge. Pre-exposure BiIA-SG injection prevents productive viral infection in 6 of 6 CRMs with unmeasurable proviral load, T cell responses, and seroconversion. Single BiIA-SG injection, at day 1 or 3 post viral challenge, significantly reduces peak viremia, achieves undetectable setpoint viremia in 8 of 13 CRMs, and delays disease progression for years in treated CRMs. In contrast, 6 of 8 untreated CRMs develop simian AIDS within 2 years. BiIA-SG-induced long-term protection is associated with $CD8^+$ T cells as determined by anti-CD8β antibody depletion experiments. Our findings provide a proof-of-concept that bi-bNAb treatment elicits T cell immunity in NHPs, which warrant the clinical development of BiIA-SG for HIV-1 prevention and immunotherapy.

INTRODUCTION

The promotion of combined antiretroviral therapy (cART) among HIV-1 infected people has resulted not only in a significant reduction of acquired immunodeficiency syndrome (AIDS)-associated mortality but also in the decrease of viral spread especially after the global efforts of treatment as prevention (Deeks et al., 2016; Brault et al., 2019). However, due to the unlikely life-long sustainable cost and compliance of cART, new approaches for preventing and curing HIV-1 remain urgently needed to fight the global HIV/AIDS pandemic (Deeks et al., 2016). Given the extreme difficulty in generating effective HIV-1 vaccines to elicit broadly neutralizing antibodies (bNAbs) in both pre-clinical and clinical studies, passive immunization using newly discovered or engineered bNAbs for HIV-1 prevention and immunotherapy has been actively explored as a promising alternative modality.

Since 2009, many potent bNAbs have been isolated directly from infected patients by the advent of single B cell sorting and cloning (Tiller et al., 2008; Smith et al., 2009; Huang et al., 2012; Seeds et al., 2011; Wu et al., 2010; Zhou et al., 2018; Huang et al., 2016a; Walker et al., 2011). Studies using non-human primates (NHP) have shown that mono or combined second-generation bNAbs prevent macaques from high-dose or serial low-dose mucosal challenges with various simian-human immunodeficiency virus (SHIV) strains. The bNAbs immunotherapy, however, only suppressed viremia transiently during chronic infection, followed by the generation of bNAbs resistant viruses or anti-drug antibodies (ADA) (Liu et al., 2016; Gautam et al., 2018; Mascola, 2002; Moldt et al., 2012; Shingai et al., 2013). One exception was that 3 out of 18 Indian-origin rhesus macaques (IRMs) remained no viral rebound for more than 100 days after receiving bNAb PGT121 treatment 9 months post-infection (Barouch et al., 2013). Moreover, combined PGT121 with toll-like receptor (TLR7) agonist vesatolimod (GS-9620) during cART delayed viral rebound and reduced viral reservoir in a subset of IRMs after cART discontinuation (Borducchi et al., 2018). Recent studies demonstrated that early short-term bNAbs treatments, given at 1–3 days post-infection (dpi),

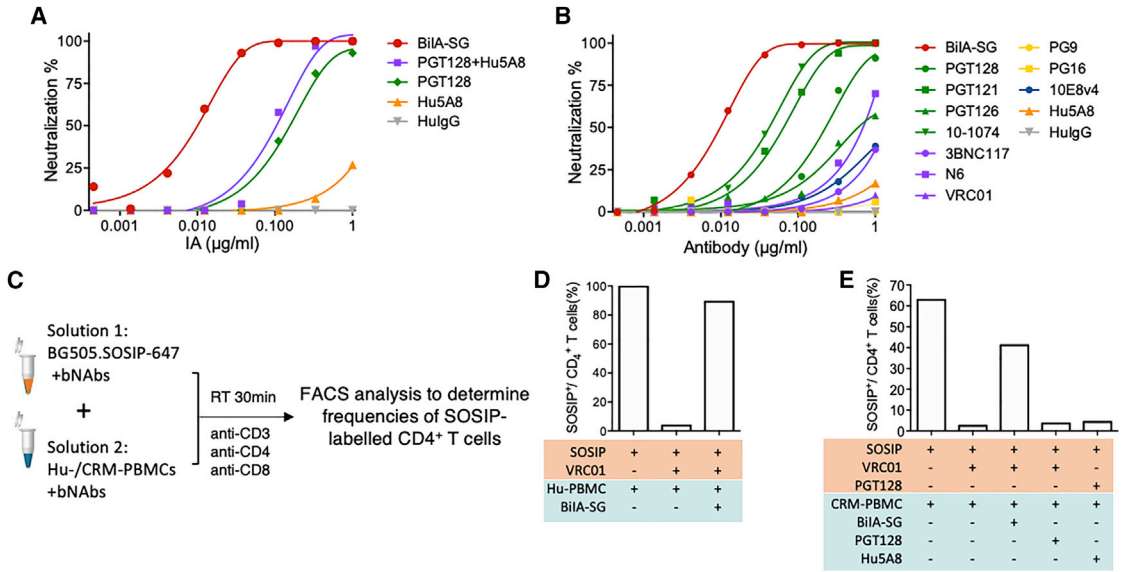

Figure 1. Characteristics of BiIA-SG *in vitro*

(A and B) Neutralization efficacy of BiIA-SG compared with its parental bNAbs (A) and a panel of bNAbs (B) against $SHIV_{SF162P3CN}$.

(C–E) Binding of soluble gp120 and CD4 molecules on $CD4^+$ T cells derived from human (Hu) or Chinese rhesus macaques (CRM) by BiIA-SG. AF647-labeled BG505.SOSIP trimer was first incubated with VRC01, PGT128, or left untreated, followed by mixing with Hu-PBMCs or CRM-PBMCs that were pretreated with BiIA-SG, PGT128, Hu5A8, or left untreated. PBMCs were then stained with anti-CD3, anti-CD4, and anti-CD8 antibodies for fluorescence-activated cell sorting (FACS) analysis. Frequencies of $SOSIP^+/CD4^+$ T cells (%) in Hu-PBMCs (D) and CRM-PBMCs (E) of different treatment groups are shown.

could block virus acquisition or achieve the sustainable control of SHIV infection (Nishimura et al., 2017; Hessell et al., 2016). It remains unknown, however, if other types of bNAbs or bi-bNAb would have similar efficacy in the SHIV/NHP models.

Besides NHP studies, some clinical trials have evaluated individual or combined anti-gp120 CD4 binding site antibody (e.g., VRC01 and 3BNC117) and anti-V3 glycan antibody (e.g., 10-1074 and PGT121) for HIV-1 prevention and immunotherapy (Gilbert et al., 2017). Consistently, bNAb monotherapy resulted in transient viral suppression among chronically infected patients, followed frequently by the occurrence of antibody-resistant viruses during viral rebound (Ledgerwood et al., 2015; Lynch et al., 2015; Bar et al., 2016; Caskey et al., 2015; Scheid et al., 2016; Caskey et al., 2017). The combined 3BNC117 and 10-1074 treatment was more effective in suppressing viremia and maintaining viral suppression for a longer period of time, especially in infected individuals with lower viremia and antibody-sensitive viral strains (Bar-On et al., 2018; Cohen et al., 2019; Mendoza et al., 2018). These findings suggest that bNAbs not only neutralize HIV-1 to suppress viremia and prevent viral acquisition but also accelerate the clearance of distal infected foci and infected cells. Although bNAb interventions during the acute phase of infection may mitigate deleterious events, attenuate the establishment of viral infection, and induce host immunity (Schoofs et al., 2016; Igarashi et al., 1999; Lu et al., 2016; Liu et al., 2016), the underlying correlates of protection remain incompletely understood.

Although some bNAb combination immunotherapies display promising efficacy in preclinical and clinical settings, bi- and tri-specific bNAbs have not been well studied in SHIV/NHP models. Based on *in vitro* experiments, bi-bNAbs and tri-bNAbs might target distinct epitopes simultaneously with extensively enhanced synergy in breadth and potency as well as in avidity (Pace et al., 2013; Huang et al., 2016b; Bournazos et al., 2016; Xu et al., 2017; Steinhardt et al., 2018; Khan et al., 2018). Some of these recombinant antibody designs might also reduce manufacturing cost, simplify treatment regimens, and avoid regulatory complicity. To date, however, only the VRC01/PGDM1400-10E8v4 tri-bNAb was able to prevent $SHIV_{BaIP4}$ and $SHIV_{325c}$ infections, yet its therapeutic potency remains elusive (Xu et al., 2017). We recently reported that a tandem bi-bNAb, BiIA-SG, which combined the anti-V3 glycan bNAb PGT128 and the humanized bNAb Hu5A8 directed to the domain 2 of human CD4, prevented diverse HIV-1 infections and eliminated infected cells by adeno-associated virus (AAV)-transferred immunotherapy in some humanized mice (Wu et al., 2018). Although humanized mice are widely used to study bNAb efficacy (Klein et al., 2012; Diskin et al., 2011), their short lifespan and lack of host immunity limit the translation of the study results for clinical development. Therefore, we sought to examine the efficacy of BiIA-SG in Chinese-origin rhesus macaques (CRMs) against the pathogenic $SHIV_{SF162P3CN}$, a CRM-adapted tier-2 R5-tropic challenge strain, aiming to obtain experimental evidence in NHPs to support clinical investigation of BiIA-SG for HIV-1 prevention and immunotherapy.

RESULTS

BiIA-SG blocks gp120 on viruses and CD4 on the surface of cells and is pharmacokinetically bioavailable in CRMs

The efficacy of bi-bNAb has not been studied in the SHIV/NHP models. In this study, we first determined the potency of BiIA-SG

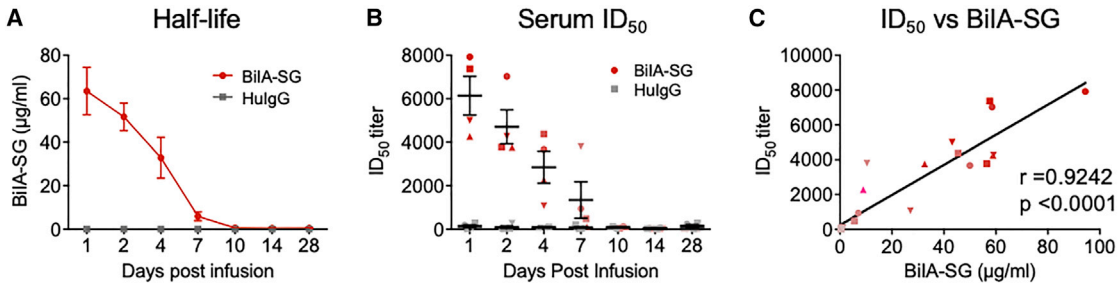

Figure 2. Pharmacokinetics and pharmacodynamics of BiIA-SG in CRMs

Four naive CRMs were injected with 10 mg/kg BiIA-SG intramuscularly, whereas the other 4 macaques were injected with 10 mg/kg HuIgG as controls.

(A) *In vivo* BiIA-SG half-life in the CRMs.

(B) *In vitro* neutralization titers (shown as ID_{50}) of sera derived from BiIA-SG-injected CRMs against $SHIV_{SF162P3CN}$.

(C) The correlation of *in vitro* ID_{50} titers and BiIA-SG concentrations among the samples collected from the 4 BiIA-SG-injected CRMs at various time points. Correlation analyses were performed by linear regression. Data are expressed as means ± SEM.

against the live pathogenic R5-tropic $SHIV_{SF162P3CN}$, which was derived from a $SHIV_{SF162P3}$-infected IRM at the end stage of simian AIDS (Harouse et al., 2001), and was subsequently adapted for growth in CRM peripheral blood mononuclear cells (PBMCs). BiIA-SG consistently exhibited the strongest potency with 50% inhibitory concentration (IC_{50}) and 90% inhibitory concentration (IC_{90}) values of 0.010 μg/mL and 0.034 μg/mL as compared with parental bNAbs PGT128 and Hu5A8 or their combination (Figure 1A). PGT128 displayed IC_{50} and IC_{90} values of 0.156 μg/mL and 0.567 μg/mL, respectively, whereas Hu5A8 showed barely any neutralizing activity because it did not have direct neutralizing effect on the virus. BiIA-SG, therefore, had a greatly enhanced neutralizing ability (15.6-fold of IC_{50} and 16.7-fold of IC_{90}) as compared to PGT128. This finding suggested that the anchoring of BiIA-SG via CD4 on target cells may ambush the invading viruses more effectively (Huang et al., 2016b; Wu et al., 2018). Moreover, by testing a large panel of bNAbs, $SHIV_{SF162P3CN}$ is susceptible to the neutralization of bNAbs mainly directed to V3 glycan (e.g., 10-1074, PGT121, and PGT126) but not to other regions (Figure 1B), which is similar to the phenotype of the parental $SHIV_{SF162P3}$ strain (Hsu et al., 2003; Julg et al., 2017b).

BiIA-SG has the same two complete binding domains as each of its parental bNAbs. This design protects the binding avidity of two PGT128 arms, allowing the possible intra-trimer or inter-trimer interaction as suggested previously (Wu et al., 2018; Ferrari, 2018). However, the binding affinity of BiIA-SG to CD4 molecule is reduced ~229-fold when compared with the parental Hu5A8 antibody (Wu et al., 2018). For this reason, we sought to determine how BiIA-SG interacts with both rhesus CD4 molecule and HIV-1 glycoprotein using the fluorescence-labeled BiIA-SG and BG505 SOSIP trimer for detection. We found that BiIA-SG binds to both human and rhesus CD4 molecules on primary $CD4^+$ T cells by flow cytometry (Figure S1). Moreover, BiIA-SG was able to bridge the binding to the V3 glycan domain on the BG505 SOSIP trimer after its binding site to human or CRM CD4 was completely blocked by the VRC01 antibody (Figures 1C–1E). These results demonstrated that BiIA-SG blocks two portals of viral entry, the V3 glycan domain on the virus and the CD4 molecule on the target cell simultaneously, as a mode of action.

We then inoculated intramuscularly 10 mg/kg BiIA-SG into 4 naive CRMs. Animal plasma samples were collected over time for measuring BiIA-SG pharmacokinetics and bioavailability against $SHIV_{SF162P3CN}$. Although the calculated peripheral half-life of BiIA-SG was 2.34 days, the antiviral plasma concentration could maintain above 1 μg/mL for around 7–10 days (Figure 2A). There was a strong positive correlation between plasma BiIA-SG concentration and neutralizing titer against $SHIV_{SF162P3CN}$ (Figures 2B and 2C). These results indicated that the engineered BiIA-SG displays potent anti-$SHIV_{SF162P3CN}$ activities *ex vivo* and the intramuscular injection is practical, allowing its bio-distribution in CRMs from the site of administration into lymphatic drainage and peripheral blood similar to conventional antibodies (Zhao et al., 2013; Ryman and Meibohm, 2017).

High-dose intravenous $SHIV_{SF162P3CN}$ challenge results in high mortality in CRMs

To determine the potency of BiIA-SG in the $SHIV_{SF162P3CN}$/CRM model, we conducted pre-exposure and post-exposure experiments with a total of 27 CRMs. In two experiments, a total of 8 CRMs (group A, A1–A8) were challenged intravenously by $SHIV_{SF162P3CN}$ alone at a high-dose of 5,000 tissue infectious dose 50 ($TCID_{50}$) (Figure 3A). All CRMs were infected, reaching the peak viremia to 1.8×10^7 copies/mL on average within 10–14 dpi (Figure 3B). Strikingly, although 8 of 8 (100%) CRMs displayed persistent high viremia, 6 of 8 (75%) infected CRMs developed the CD4/CD8 ratio drop (Figure 3C), progressive diarrhea, anorexia, body weight loss, and subsequent progression to death (Figure 3D). During the experimental period, only 2 surviving macaques displayed anti-$HIV\text{-}1_{SF162}$ gp120 humoral response after 42 dpi (Figure 3E). Therefore, we demonstrated that high-dose intravenous challenge of the CRM-adapted R5-tropic $SHIV_{SF162P3CN}$ led to persistent infection, simian AIDS, and high mortality in the majority of CRMs.

Prior BiIA-SG injection confers protection against high-dose intravenous $SHIV_{SF162P3CN}$ infection

To determine if the prophylactic injection of BiIA-SG would prevent viral infection in NHPs, we inoculated 6 CRMs (group B) with 10 mg/kg BiIA-SG either intramuscularly (B1–B3) or

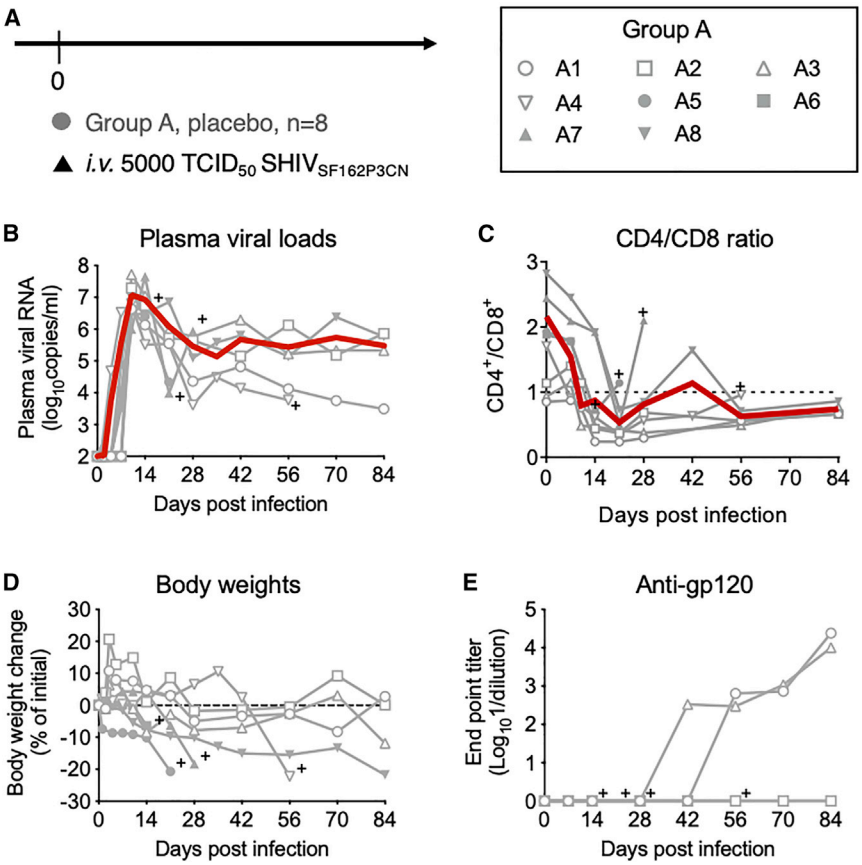

Figure 3. Pathogenicity of high-dose intravenous SHIV$_{SF162P3CN}$ challenge in CRMs

(A) Establishment of SHIV$_{SF162P3CN}$ infection in CRMs. A group of 8 CRMs were intravenously challenged with 5,000 TCID$_{50}$ SHIV$_{SF162P3CN}$.

(B–E) Characterization of high-dose intravenous (i.v.) SHIV$_{SF162P3CN}$ challenge in CRMs without treatment (gray, group A). (B) Kinetics of plasma viral loads were determined over time. The red line represents the mean log RNA copies/mL. (C) CD4/CD8 T cell ratios were measured in CRM peripheral blood over time. The red line represents the mean CD4/CD8 T cell ratio. (D) Body weight changes were measured after SHIV$_{SF162P3CN}$ challenge. (E) Endpoint titers of anti-HIV-1$_{SF162}$ gp120 antibody were determined by ELISA in animal plasma samples over time. CRMs that were euthanized during the experimental period were marked with +.

intravenously (B4–B6) 24 h before the intravenous SHIV$_{SF162P3CN}$ challenge (Figure 4A). As compared to the untreated CRMs in group A (A1–A8), there was no productive plasma viral RNA detected longitudinally after the challenge among 6 of 6 (100%) CRMs in group B (Figure 4B). A minor viral blip was detected in one animal initially, but importantly, all animals showed no detectable plasma viral load subsequently. The CD4/CD8 ratios were fluctuated initially but stabilized 28 dpi in group B CRMs (Figure 4C). Consistent to the pharmacokinetic experiment, plasma BiIA-SG maintained at levels exceeding the *in vitro* neutralization IC$_{50}$ value against SHIV$_{SF162P3CN}$ for around 7–14 dpi (Figure 4D). Interestingly, the average half-life of BiIA-SG in the challenged animals is 1.32 days, shorter than those measured in antibody treated but uninfected animals (Figure 2A). Virions might adsorb some amounts of BiIA-SG in these challenged animals. Proviral DNA loads remained undetectable over 12 weeks in 6 of 6 (100%) group B CRMs by digital PCR (Figure 4E). In addition, Env-specific humoral responses and T cell responses against viral Gag and Nef were also undetectable in these CRMs (Figure 4F and 4G). Although antibody injected intravenously might have less on-site loss and faster bioavailability (Miller et al., 2005; Liu et al., 2016), prior intramuscular injection of BiIA-SG is equally effective in preventing high-dose pathogenic SHIV$_{SF162P3CN}$ infection in CRMs. Collectively, our results demonstrated that there was lack of productive infection in all BiIA-SG pre-treated macaques.

Post-exposure BiIA-SG converts pathogenic SHIV$_{SF162P3CN}$ infection into long-term viremia control

A previous NHP study showed that cART, as early as 3 dpi, was too late to stop the rapid viral reservoir seeding as evidenced by the viral rebound after treatment disruption (Whitney et al., 2014). We sought to investigate if post-exposure BiIA-SG monotherapy at 1 dpi and 3 dpi would prevent latency establishment and SHIV$_{SF162P3CN}$ infection. After the intravenous SHIV$_{SF162P3CN}$ challenge, a single injection of 20 mg/kg BiIA-SG was administrated intramuscularly on 1 dpi for 7 CRMs in group C and on 3 dpi for 6 CRMs in group D (Figure 5A). All 13 macaques became infected, reaching their plasma viral RNA load peaks from 14 to 28 dpi (Figures 5B and 5C). Their CD4/CD8 ratio dropped during peak viremia and then stabilized (Figures 5D and 5E). Importantly, none of the treated CRMs developed progressive diarrhea, body weight loss, or significant CD4 lymphocytopenia. In addition, there were significantly decreased peak viral loads in group D CRMs (Figure 5F), postponed date of peak viremia occurrence (Figure 5G), as well as reduced set-point viral RNA and proviral loads (Figures 5H and 5I) in both C and D groups, as compared to the untreated CRMs in group A. Most importantly, the single-dose of BiIA-SG post-exposure treatment saved 13 of 13 (100%) infected CRMs from death with a significant survival advantage (Figure 5J). Crucially, 8 of 13 (61.5%) treated CRMs became controllers with undetectable plasma viral loads around 84 dpi, including 5 of 7 (71.4%) in group C and 3 of 6 (50%) in group D. The rest of the 5 CRMs in these two groups were considered as non-controllers. These results demonstrated that although single intramuscular injection of BiIA-SG did not achieve complete post-exposure prevention even administrated at 1 dpi, this treatment could actively suppress pathogenic infection and prevent disease progression in all 13 BiIA-SG-treated CRMs.

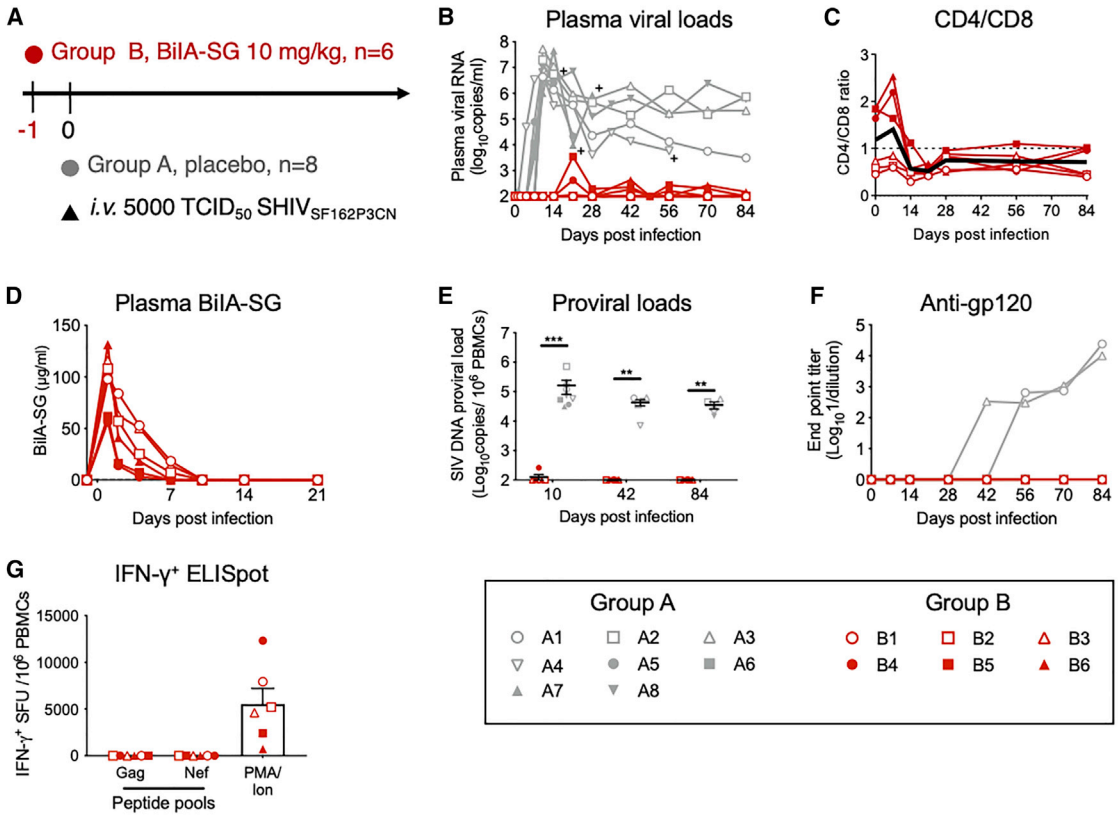

Figure 4. Protection against pathogenic $SHIV_{SF162P3CN}$ challenge by BiIA-SG pre-treatment

(A) Experimental schedule of BiIA-SG pre-treatment against pathogenic $SHIV_{SF162P3CN}$ infection. A group of 6 CRMs were pre-treated with BiIA-SG (10 mg/kg) via intramuscular (B1-B3) or intravenous (B4-B6) injection, followed by i.v. challenge with the 5,000 $TCID_{50}$ of $SHIV_{SF162P3CN}$ 1 day later (red, group B).

(B) Kinetics of plasma viral loads were compared with CRMs in group A.

(C) CD4/CD8 T cell ratios were determined in peripheral blood over time. The black line represents the mean CD4/CD8 T cell ratio.

(D) BiIA-SG concentrations were determined in plasma.

(E) Proviral DNA loads were determined in PBMCs.

(F) Endpoint titers of anti-$HIV\text{-}1_{SF162}$ gp120 antibody were determined in plasma over time.

(G) T cell responses were measured by IFN-γ^+ ELISpot assay against viral Gag and Nef overlapping peptide pools at 8 weeks post-challenge. PMA/ionomycin (PMA/ion) was included as a positive control for each sample. CRMs that were euthanized during the experimental period were marked with +. Data are expressed as means ± SEM. Significance of differences was determined by Wilcoxon rank-sum test. *$p < 0.05$; **$p < 0.01$, ***$p < 0.001$.

Possible mechanisms underlying BiIA-SG-mediated long-term viremia control

To investigate BiIA-SG-mediated protection among the treated CRMs, we first measured peripheral BiIA-SG concentration. Consistently, the infused BiIA-SG maintained for 7–14 days in plasma (Figure 6A). The short half-life of BiIA-SG was found due to the rapid development of ADA response because BiIA-SG, as a human bi-bNAb, was immunogenic in CRMs (Figures 6A and S2). $HIV\text{-}1_{SF162}$ gp120-specific humoral responses were induced after 28 dpi and remained at high levels (Figures 6B and S2). In contrast, all CRMs in groups C and D did not develop autologous neutralizing antibodies (ID_{80} <1:100) against $SHIV_{SF162P3CN}$ within 84 dpi (Figure 6C). The early neutralization activity detected in the plasma of the BiIA-SG-treated animals within the first 3 weeks post-challenge was caused by the presence of BiIA-SG. Env- and Gag-specific T cell responses, however, were elicited in the treated CRMs (Figures 6D and 6E).

Because there were no measurable autologous NAbs within 3 months of infection, we determined the protective role of $CD8^+$ T cells in mediating the sustained viral suppression by administering the CD8 T cell depleting anti-CD8β monoclonal antibody (mAb), which targets more specifically $CD8^+$ T cells than anti-CD8α mAb (Nishimura et al., 2017) in four controllers (C2, C3, D2, and D3) as compared with the other four controllers (C1, C5, C6, and D1). Although the infusion of anti-CD8β mAb led to a moderate decline of $CD8^+$ T cells (Figure S3A), it resulted in the immediate rebound of plasma viral loads in all 4 tested CRMs (Figure 7A). After viremia returned to undetectable levels 6 weeks after the injection of anti-CD8β mAb, two CRMs, C2 and D2, underwent viral rebounds once and twice on 210 dpi and 327 dpi, respectively, eventually resulting in wasting and death. Envelope sequences of peripheral rebound viruses by single genome analysis (SGA) did not reveal any X4-tropic or PGT-128 resistant variants (Figure S3B). The remaining 4 controllers (C1, C5, C6, and D1), which did not receive anti-CD8β mAb, displayed sustainable

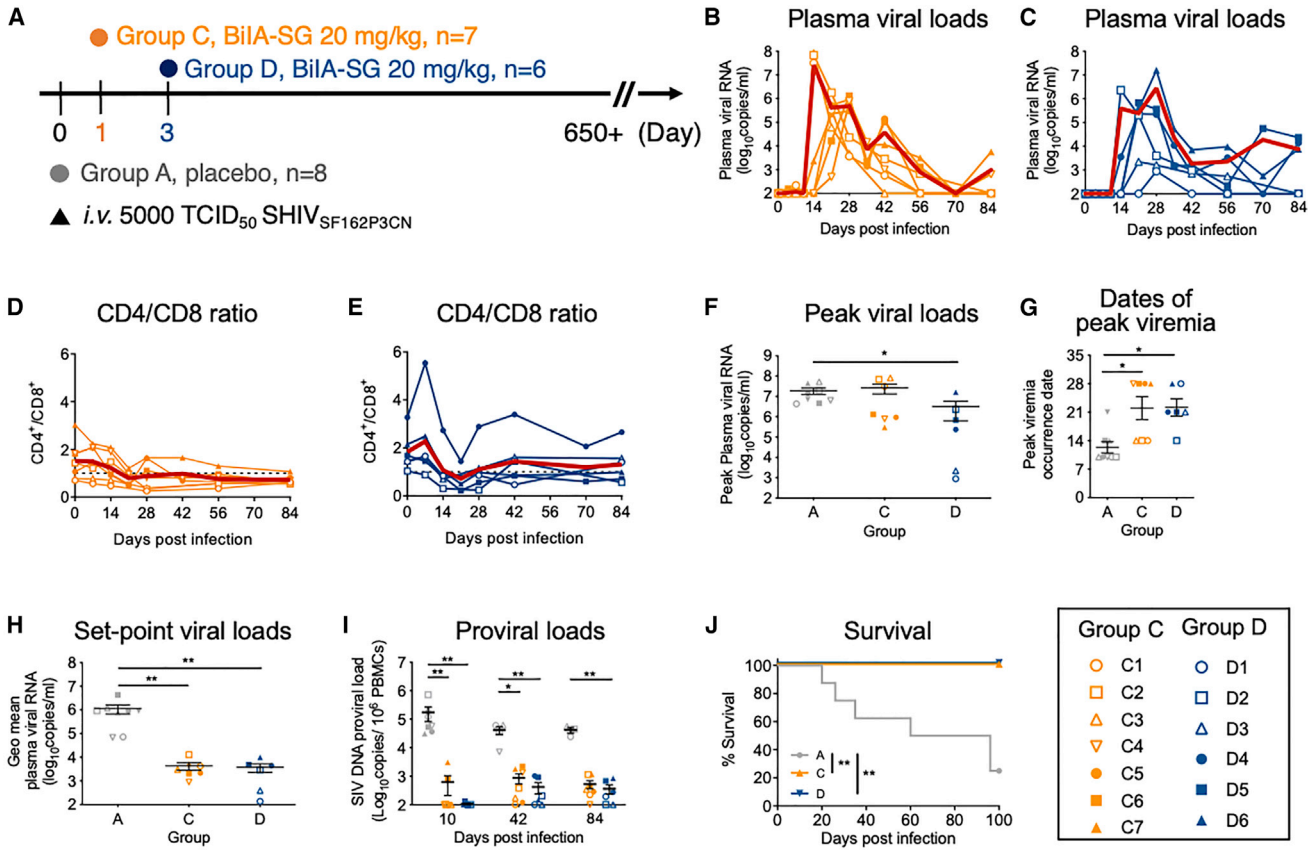

Figure 5. Protective efficacy of early BilA-SG treatment against $SHIV_{SF162P3CN}$ challenge

(A) Experimental schedule of early BilA-SG treatment against $SHIV_{SF162P3CN}$ infection. CRMs were challenged with 5,000 $TCID_{50}$ of $SHIV_{SF162P3CN}$ intravenously, followed by intramuscular BilA-SG treatment (20 mg/kg) at 1 dpi (orange, group C; n = 7) or 3 dpi (blue, group D; n = 6).

(B and C) Kinetics of plasma viral loads were determined in group C (B) and group D (C). Mean plasma viral load kinetics was shown as a red line for each group.

(D and E) CD4/CD8 T cell ratios were determined in peripheral blood from group C (D) and group D (E). The red line represents the mean CD4/CD8 T cell ratio.

(F) Comparison of peak viremia levels was made among different treatment groups.

(G) Comparison of peak viremia occurrence date was made post-infection.

(H) Setpoint viral loads were determined in peripheral blood samples. Geometric means were calculated for each macaque based on the viral loads between 14–84 days post-challenge.

(I) Proviral DNA loads were determined in PBMCs at the indicated time points.

(J) Precent survival was determined for BilA-SG treated and untreated CRMs. Data are expressed as means ± SEM for each group. Statistical significance was determined by the Wilcoxon rank-sum test (F–I) or the log-rank test (J). *$p < 0.05$; **$p < 0.01$, ***$p < 0.001$.

viremia control except for one animal (C1) that had low levels of viral blips on 385 and 432 dpi (Figure 7B). These findings demonstrated that $CD8^+$ T cells played critical roles in the control of viral replication in controller CRMs.

Although plasma viral loads fluctuated at various levels among five non-controllers (C4, C7, D4, D5, and D6), these CRMs survived for 649 dpi without any sign of simian AIDS (Figure 7C). We measured T cell responses from 4 and 3 macaques from groups C and D, respectively, at the later phase post viral challenge at 503 dpi. They developed long-term anti-Gag and Nef memory T cell responses (Figures S4A–S4E). There was a trend of higher $CD4^+$ T cell responses against Gag and Nef in non-controllers than controllers (Figure S4F). In comparison, levels of Gag- and Nef-specific $CD8^+$ T cell responses varied among the macaques. Moreover, there was a significant positive correlation of plasma viral loads to Nef-specific $CD4^+$ T cells and a trend of positive association of plasma viral loads to Gag-specific $CD4^+$ T cells, suggesting that active viral replication might activate $CD4^+$ T cells. In comparison, there was no clear correlation of viral loads to the levels of viral-specific $CD8^+$ T cell responses at the time of measurement (Figure S4G). Interestingly, when we continuously measured their antibody responses, all macaques had high autologous gp120 binding antibody titers (Figure S5). Four of eight controller CRMs with either anti-CD8β-induced (3 of 4) or spontaneous viral replication (1 of 4) developed autologous NAbs (Figures 7D and 7E). Similarly, 4 of 5 non-controller CRMs with active viral loads also developed autologous NAbs against the challenge virus (Figure 7F). In comparison, most of the CRMs in group A did not survive past 12 weeks post-challenge, and a much lower autologous NAb activity was detected from these animals (Figure 7G). Moreover, we found that controller CRMs had less CD4/CD8 ratio decrease as compared with

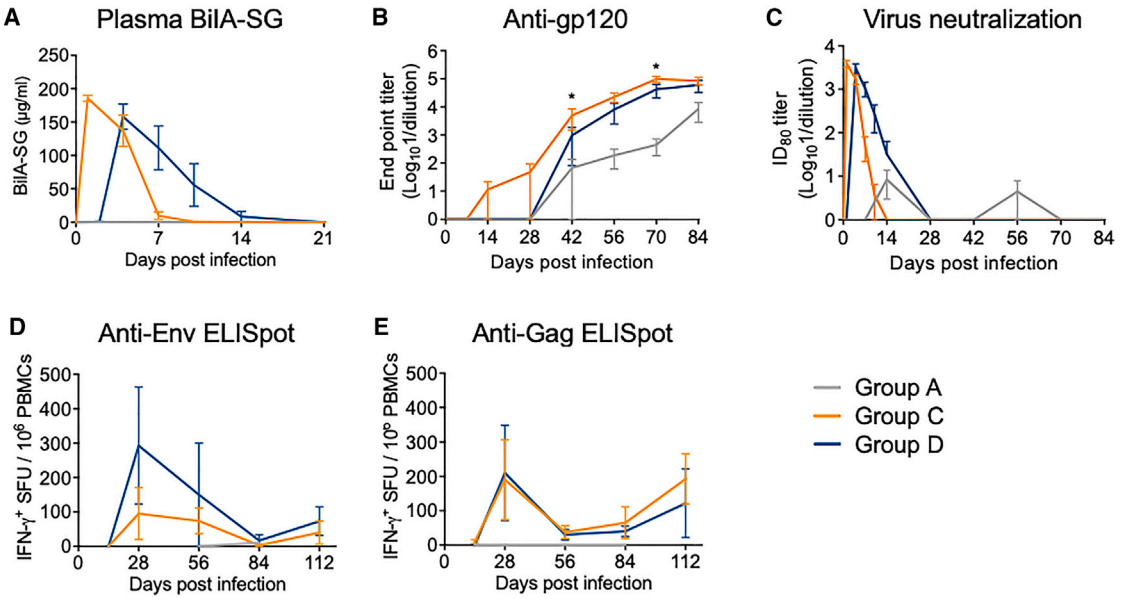

Figure 6. Induction of humoral and cellular responses by early BiIA-SG treatment against $SHIV_{SF162P3CN}$ challenge

(A) Plasma BiIA-SG concentrations were measured for CRMs in groups C and D over time post viral infection.

(B) Endpoint titers of anti-$HIV\text{-}1_{SF162}$ gp120 antibody were determined for CRMs in groups A, C, and D.

(C) Plasma neutralization titers were determined against challenge virus stock $SHIV_{SF162P3CN}$.

(D and E) T cell responses were measured by the IFN-γ^+ ELISpot assay in PBMCs against Env (D) and Gag (E) antigens. Data are expressed as means ± SEM. Statistical significance was determined by the Wilcoxon rank-sum test. *$p < 0.05$.

untreated and non-controller CRMs within 3 months of infection, indicating better preservation of CD4 T cells by early BiIA-SG treatment (Figure 7H). Our results demonstrated that BiIA-SG treatment might be able to trigger germline NAb response, which was boosted subsequently by viral replication.

DISCUSSION

Here, we presented what is, to the best of our knowledge, the first study on a bi-bNAb in a pathogenic SHIV/NHP model for both prophylactic and immunotherapeutic efficacy. We showed that BiIA-SG could block two portals of viral entry simultaneously, allowing anchoring of the tandem bispecific antibody via CD4 on target cells to block the invading viruses with greatly enhanced potency and breadth (Huang et al., 2016b; Wu et al., 2018). We also demonstrated that single intramuscular or intravenous injection not only made BiIA-SG bioavailable pharmacokinetically, but also prevented pathogenic $SHIV_{SF162P3CN}$ infection in CRMs under pre-exposure conditions with undetectable or very low levels of plasma viral RNA, cell-associated proviral DNA or seroconversion. Furthermore, although single intramuscular injection of BiIA-SG did not achieve post-exposure prevention even administrated at 1 dpi, the BiIA-SG treatment suppressed pathogenic $SHIV_{SF162P3CN}$ infection and prevented disease progression to simian AIDS in treated CRMs, as compared to 6 rapid progressors in the 8 untreated CRMs in the control group. Mechanistically, we found that post-exposure BiIA-SG promoted the induction of protective $CD8^+$ T cells for durable viral suppression and development of NAbs in many antibody-treated CRMs, which were determined by CD8+T cell depleting antibody and longitudely plasma neutralizing activities, respectively. Since it is feasible to produce BiIA-SG under GMP conditions, our findings warrant its clinical investigation for HIV-1 prevention and immunotherapy.

CRMs infected intravenously with the high dose of pathogenic $SHIV_{SF162P3CN}$ did not progress spontaneously into controllers with undetectable viral loads, but rather into progressors with persistent viremia and subsequent simian AIDS. In this study, we generated our $SHIV_{SF162P3CN}$ challenge stock using CRM PBMCs, which is different from the $SHIV_{SF162P3}$ challenge stock obtained directly from the NIH reagent program. $SHIV_{SF162P3}$ as a tier-2 virus has been extensively used for various vaccine and antibody efficacy studies primarily using IRMs (Shingai et al., 2013; Hessell et al., 2016; Liu et al., 2016; Julg et al., 2017a; Nishimura et al., 2017; Xu et al., 2017; Gautam et al., 2018). There was a concern that CRMs infected by IRM-PBMC derived $SHIV_{SF162P3}$ might progress spontaneously into controllers and, therefore, were not suitable for vaccine and immunotherapeutic studies. Using the CRM-adapted pathogenic $SHIV_{SF162P3CN}$, we demonstrated that none of the infected CRMs became spontaneous viremia controllers. Instead, although all 8 infected CRMs developed persistent infections, 6 of them progressed into simian AIDS with weight loss, diarrhea, anorexia, and gradual CD4 lymphocytopenia. This finding validates the practice of host cell-adaptation for enhanced viral pathogenicity probably by avoiding adaptive immune responses against cellular components in challenge virions derived from a different host species (Chen, 2018).

Post-exposure BiIA-SG monotherapy results in significantly prolonged viremia control and survival. A previous study

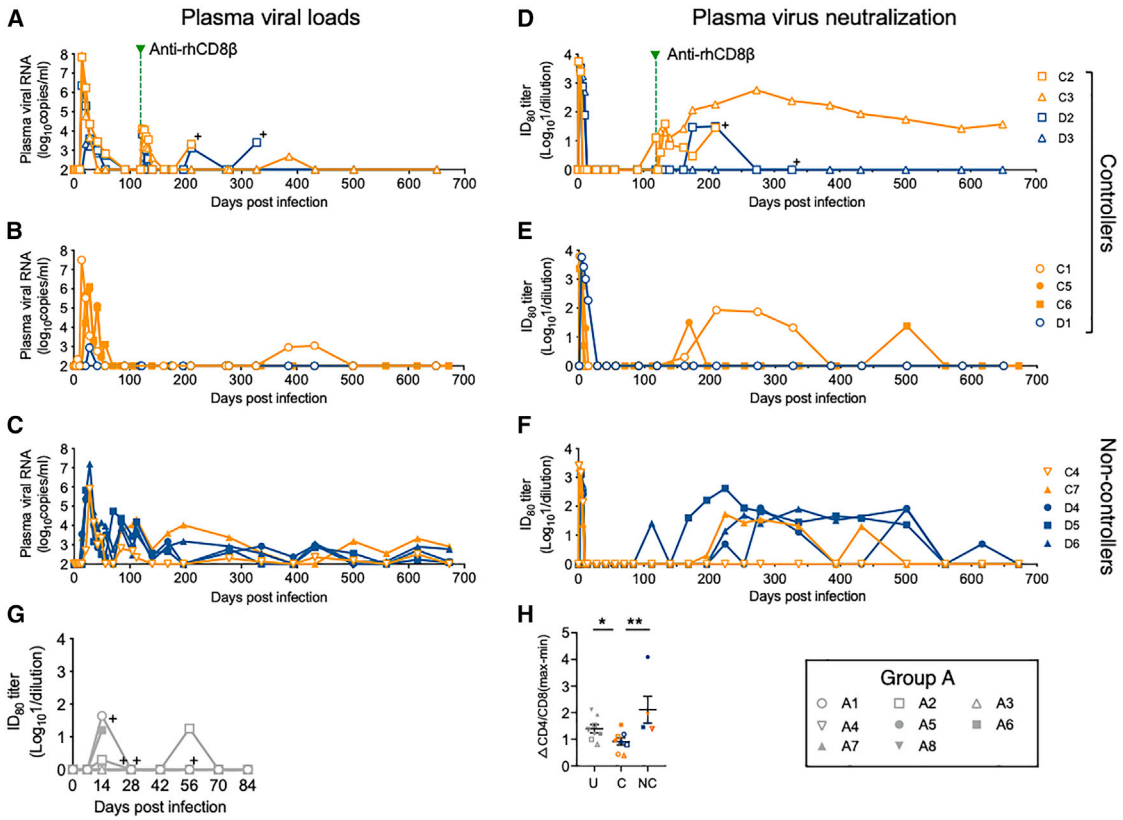

Figure 7. Long-term virological and humoral effect of early BilA-SG treatment against $SHIV_{SF162P3CN}$ challenge

(A–C) Plasma viral RNA loads were monitored up to 649 days post-infection in CRMs, including (A) 4 controller CRMs (C2, C3, D2, and D3) that received the anti-CD8β depleting antibody CD8b255R1 at day 119, (B) 4 controller CRMs (C1, C5, C6, and D1) without the CD8b255R1 treatment, and (C) 5 non-controller CRMs (C4, C7, D4, D5, and D6).

(D–G) Plasma neutralization ID_{80} titers were determined against the challenge $SHIV_{SF162P3CN}$ stock for CRMs, including 4 controller CRMs that received anti-CD8β depleting antibody (D), 4 controller CRMs without the CD8b255R1 treatment (E), 5 non-controller CRMs (F), and 8 control CRMs (G).

(H) The changes of CD4/CD8 ratios were determined in untreated (U), controller (C), and non-controller (NC) CRMs within 84 days of infection. Data are shown as means ± SEM. Statistical significance was determined by the Wilcoxon rank-sum test. *$p < 0.05$; **$p < 0.01$.

demonstrated that 2-week immunotherapy starting at 3 dpi with three consecutive doses of cocktail bNAbs (3BNC117 and 10-1074) could facilitate the induction of potent $CD8^+$ T cell immunity to convert the acute SHIV infection into prolonged control in ~50% of the macaques examined (Nishimura et al., 2017). Moreover, a short-term combinational bNAb immunotherapy provided as early as 1 dpi halted oral $SHIV_{SF162P3}$ infection in infant macaques, showing that bNAbs are effectively involved in the clearance of infectious virus in blood and distal tissues during the earliest stage of HIV penetration (Liu et al., 2016; Hessell et al., 2016). However, bNAb treatment combined with cART starting at 10 dpi could not induce viral remission (Bolton et al., 2015). Before our study, it remained unknown if a bi-specific bNAb would achieve similar antiviral immunity in NHPs. Using a different NHP species, we showed that a single post-exposure BilA-SG injection even as early as 1 dpi did not prevent the establishment of viral infection in all CRMs, despite delayed and reduced peak and set-point viremia as well as decreased proviral loads. This result was likely related mainly to two factors. One was the high dose of intravenous viral challenge used in our study because this might promote the rapid establishment of viral reservoir and make it more difficult for the post-exposure treatment as compared to low dose mucosal challenge regime. The other factor was the short half-life of BilA-SG in CRMs. This was at least partially due to the rapid induction of ADA. This outcome also prevented us from doing repeated injections of BilA-SG for immunotherapy. Importantly, the post-exposure BilA-SG monotherapy resulted in the induction of protective host immunity that led to complete plasma viral control in 8 of 13 treated CRMs and prevented all 13 treated CRMs from fatal disease progression. This was in great contrast to the occurrence of 6 rapid progressors and deaths in the 8 untreated CRMs. A reduced provirus load (in PBMCs) could explain that the treatment had limited the potential viral reservoir size, which could cause decreased pathogenesis and a better-preserved immunity. Moreover, prolonged viral control was achieved in 11 of 13 BilA-SG-treated CRMs for 649 days with the exception of 2 deaths due to viral bound and clinical wasting after the $CD8^+$ T cell depletion.

BilA-SG-mediated induction of protective immune responses is essential for immunotherapeutic efficacy. Similar to previous studies, we found that BilA-SG-treated CRMs elicited generally

earlier and higher cellular and humoral responses compared to untreated CRMs. On one hand, we verified the T cell function in viremia control directly by infusing $CD8^+$ T cell depleting antibody into 4 of 8 controller CRMs when they had not developed autologous NAbs at the time of anti-CD8β treatment. These results indicated that $CD8^+$ T cells might indeed play a significant role in controlling viremia and disease progression. These findings also indicate that latent reservoirs remain in controller CRMs. On the other hand, by monitoring adaptive humoral responses, we found that anti-gp120 antibody titer and the autologous neutralizing activity of monkey plasma was unlikely correlated with plasma viral load control. This finding might be related to virus-NAb co-evolution because higher levels of autologous NAbs against the challenge stock were found in non-controllers having persistently low viral loads, as compared to controllers. Because autologous NAbs were barely found in untreated progressor CRMs as compared with BiIA-SG-treated CRMs, BiIA-SG treatment clearly promoted the induction of NAbs. Previous studies showed that bNAb-HIV-1 immune complexes may mediate host immunity as immunoregulators (Wen et al., 2016), and future studies should investigate if BiIA-SG immune complexes are actually involved in the induction of protective immune responses, especially of bNAbs. Moreover, the early treatment of BiIA-SG likely reduced the loss of CD4 T cells in acute phase of infection, which probably also protected T follicular helper (T_{FH}) cells (Yamamoto et al., 2015). Future studies should also investigate how passive immunization of bispecific antibody preserves the T_{FH} cells. Since the CD4 binding affinity of BiIA-SG was reduced by 229-fold (Wu et al., 2018), there was unlikely a major CD4 depletion during single intramuscular injection. BiIA-SG Fc-mediated effector functions, including antibody-dependent cell cytotoxicity (ADCC) and antibody-dependent cell phagocytosis (ADCP), still should be investigated in the future (Parsons et al., 2019; Hessell et al., 2007).

One limitation for BiIA-SG clinical development is its short half-life in CRMs, which is similar to that in humanized mice (Wu et al., 2018). We found that the short half-life in CRMs might be due to fairly rapid ADA responses. As an engineered bi-bNAb for human use, this problem may be relieved when BiIA-SG is tested in human trials. We will monitor ADA responses in future human studies because the immunogenicity of engineered human antibodies has been documented in some human subjects (Caskey et al., 2015, 2017). Meanwhile, we may introduce two amino acid substitutions, lysine-serine (LS) mutation (M428L and N434S mutation), in the crystallizable fragment (Fc) domain of BiIA-SG, which could increase not only the antibody binding to neonatal Fc receptor (FcRn) for prolonged half-life but also improve its distribution into gut mucosal tissues (Ko et al., 2014). The bioavailability and efficacy of these BiIA-SG variants are currently being evaluated. Future testing of BiIA-SG in intrarectal $SHIV_{SF162P3CN}$ challenge will be needed to demonstrate the potency of this antibody drug against mucosal infection.

STAR★METHODS

Detailed methods are provided in the online version of this paper and include the following:

SUPPLEMENTAL INFORMATION

Supplemental information can be found online at https://doi.org/10.1016/j.celrep.2021.109611.

ACKNOWLEDGMENTS

We wish to thank C. Cheng-Mayer for the parental $SHIV_{SF162P3}$ viral stock and critical discussions. We thank David Ho and Kwok-Yung Yuen for scientific advice. This work and our members were supported by research grants from the Hong Kong Research Grant Council (TRS: T11-706/18-N, ANR/RGC: A-HKU709/14, GRF: 762712, CRF: HKU5/CRF/13G), The China Major Research Program on Infectious Diseases (2017ZX10201101-004), the Hong Kong Health and Medical Research Fund (17160762), University Development Fund and Li Ka Shing Faculty of Medicine Matching Fund from the University of Hong Kong to AIDS Institute, and the San-Ming Project of Medicine in Shenzhen (AR160087), People's Republic of China.

AUTHOR CONTRIBUTIONS

Z.C. contributed to conceptualization and project coordination. M.N., Y.C.W., H.W., and Z.C. designed and supervised the study. M.N., Y.C.W., X.L., C.Y.C., Q.Z., L.L., Y.D., L.C., R.W., L.Y.Y., and H.Z. performed the experiments. M.N., Y.C.W., X.L., C.Y.C., and Z.C. analyzed the data. Q.Z. and L.Z. provided reagents. X.J. coordinated the bioreactor production. M.N., Y.C.W., L.Z., and Z.C. wrote the manuscript.

DECLARATION OF INTERESTS

Z.C. and H.W. are co-inventors of BiIA-SG.

Received: October 6, 2020
Revised: April 16, 2021
Accepted: August 5, 2021
Published: August 24, 2021

REFERENCES

Bar, K.J., Sneller, M.C., Harrison, L.J., Justement, J.S., Overton, E.T., Petrone, M.E., Salantes, D.B., Seamon, C.A., Scheinfeld, B., Kwan, R.W., et al. (2016). Effect of HIV Antibody VRC01 on Viral Rebound after Treatment Interruption. N. Engl. J. Med. *375*, 2037–2050.

Bar-On, Y., Gruell, H., Schoofs, T., Pai, J.A., Nogueira, L., Butler, A.L., Millard, K., Lehmann, C., Suárez, I., Oliveira, T.Y., et al. (2018). Safety and antiviral

activity of combination HIV-1 broadly neutralizing antibodies in viremic individuals. Nat. Med. *24*, 1701–1707.

Barouch, D.H., Whitney, J.B., Moldt, B., Klein, F., Oliveira, T.Y., Liu, J., Stephenson, K.E., Chang, H.W., Shekhar, K., Gupta, S., et al. (2013). Therapeutic efficacy of potent neutralizing HIV-1-specific monoclonal antibodies in SHIV-infected rhesus monkeys. Nature *503*, 224–228.

Bolton, D.L., Pegu, A., Wang, K., McGinnis, K., Nason, M., Foulds, K., Letukas, V., Schmidt, S.D., Chen, X., Todd, J.P., et al. (2015). Human Immunodeficiency Virus Type 1 Monoclonal Antibodies Suppress Acute Simian-Human Immunodeficiency Virus Viremia and Limit Seeding of Cell-Associated Viral Reservoirs. J. Virol. *90*, 1321–1332.

Borducchi, E.N., Liu, J., Nkolola, J.P., Cadena, A.M., Yu, W.H., Fischinger, S., Broge, T., Abbink, P., Mercado, N.B., Chandrashekar, A., et al. (2018). Antibody and TLR7 agonist delay viral rebound in SHIV-infected monkeys. Nature *563*, 360–364.

Bournazos, S., Gazumyan, A., Seaman, M.S., Nussenzweig, M.C., and Ravetch, J.V. (2016). Bispecific Anti-HIV-1 Antibodies with Enhanced Breadth and Potency. Cell *165*, 1609–1620.

Brault, M.A., Spiegelman, D., Hargreaves, J., Nash, D., and Vermund, S.H. (2019). Treatment as Prevention: Concepts and Challenges for Reducing HIV Incidence. J. Acquir. Immune Defic. Syndr. *82* (*Suppl 2*), S104–S112.

Caskey, M., Klein, F., Lorenzi, J.C., Seaman, M.S., West, A.P., Jr., Buckley, N., Kremer, G., Nogueira, L., Braunschweig, M., Scheid, J.F., et al. (2015). Viraemia suppressed in HIV-1-infected humans by broadly neutralizing antibody 3BNC117. Nature *522*, 487–491.

Caskey, M., Schoofs, T., Gruell, H., Settler, A., Karagounis, T., Kreider, E.F., Murrell, B., Pfeifer, N., Nogueira, L., Oliveira, T.Y., et al. (2017). Antibody 10-1074 suppresses viremia in HIV-1-infected individuals. Nat. Med. *23*, 185–191.

Chen, Z. (2018). Monkey Models and HIV Vaccine Research. Adv. Exp. Med. Biol. *1075*, 97–124.

Chung, H.-K., Unangst, T., Treece, J., Weiss, D., and Markham, P. (2008). Development of real-time PCR assays for quantitation of simian betaretrovirus serotype-1, -2, -3, and -5 viral DNA in Asian monkeys. J. Virol. Methods *152*, 91–97.

Cline, A.N., Bess, J.W., Piatak, M., Jr., and Lifson, J.D. (2005). Highly sensitive SIV plasma viral load assay: practical considerations, realistic performance expectations, and application to reverse engineering of vaccines for AIDS. J. Med. Primatol. *34*, 303–312.

Cohen, Y.Z., Butler, A.L., Millard, K., Witmer-Pack, M., Levin, R., Unson-O'Brien, C., Patel, R., Shimeliovich, I., Lorenzi, J.C.C., Horowitz, J., et al. (2019). Safety, pharmacokinetics, and immunogenicity of the combination of the broadly neutralizing anti-HIV-1 antibodies 3BNC117 and 10-1074 in healthy adults: A randomized, phase 1 study. PLoS ONE *14*, e0219142.

Deeks, S.G., Lewin, S.R., Ross, A.L., Ananworanich, J., Benkirane, M., Cannon, P., Chomont, N., Douek, D., Lifson, J.D., Lo, Y.R., et al.; International AIDS Society Towards a Cure Working Group (2016). International AIDS Society global scientific strategy: towards an HIV cure 2016. Nat. Med. *22*, 839–850.

Diskin, R., Scheid, J.F., Marcovecchio, P.M., West, A.P., Klein, F., Gao, H., Gnanapragasam, P.N., Abadir, A., Seaman, M.S., Nussenzweig, M.C., and Bjorkman, P.J. (2011). Increasing the potency and breadth of an HIV antibody by using structure-based rational design. Science *334*, 1289–1293.

Ferrari, G. (2018). Tandem bispecific broadly neutralizing antibody - a novel approach to HIV-1 treatment. J. Clin. Invest. *128*, 2189–2191.

Gautam, R., Nishimura, Y., Gaughan, N., Gazumyan, A., Schoofs, T., Buckler-White, A., Seaman, M.S., Swihart, B.J., Follmann, D.A., Nussenzweig, M.C., and Martin, M.A. (2018). A single injection of crystallizable fragment domain-modified antibodies elicits durable protection from SHIV infection. Nat. Med. *24*, 610–616.

Gilbert, P.B., Juraska, M., deCamp, A.C., Karuna, S., Edupuganti, S., Mgodi, N., Donnell, D.J., Bentley, C., Sista, N., Andrew, P., et al. (2017). Basis and Statistical Design of the Passive HIV-1 Antibody Mediated Prevention (AMP) Test-of-Concept Efficacy Trials. Stat. Commun. Infect. Dis. *9*, 20160001.

Harouse, J.M., Gettie, A., Eshetu, T., Tan, R.C.H., Bohm, R., Blanchard, J., Baskin, G., and Cheng-Mayer, C. (2001). Mucosal transmission and induction of simian AIDS by CCR5-specific simian/human immunodeficiency virus SHIV(SF162P3). J. Virol. *75*, 1990–1995.

Hessell, A.J., Hangartner, L., Hunter, M., Havenith, C.E., Beurskens, F.J., Bakker, J.M., Lanigan, C.M., Landucci, G., Forthal, D.N., Parren, P.W., et al. (2007). Fc receptor but not complement binding is important in antibody protection against HIV. Nature *449*, 101–104.

Hessell, A.J., Jaworski, J.P., Epson, E., Matsuda, K., Pandey, S., Kahl, C., Reed, J., Sutton, W.F., Hammond, K.B., Cheever, T.A., et al. (2016). Early short-term treatment with neutralizing human monoclonal antibodies halts SHIV infection in infant macaques. Nat. Med. *22*, 362–368.

Hsu, M., Harouse, J.M., Gettie, A., Buckner, C., Blanchard, J., and Cheng-Mayer, C. (2003). Increased mucosal transmission but not enhanced pathogenicity of the CCR5-tropic, simian AIDS-inducing simian/human immunodeficiency virus SHIV(SF162P3) maps to envelope gp120. J. Virol. *77*, 989–998.

Huang, J., Ofek, G., Laub, L., Louder, M.K., Doria-Rose, N.A., Longo, N.S., Imamichi, H., Bailer, R.T., Chakrabarti, B., Sharma, S.K., et al. (2012). Broad and potent neutralization of HIV-1 by a gp41-specific human antibody. Nature *491*, 406–412.

Huang, J., Kang, B.H., Ishida, E., Zhou, T., Griesman, T., Sheng, Z., Wu, F., Doria-Rose, N.A., Zhang, B., McKee, K., et al. (2016a). Identification of a CD4-Binding-Site Antibody to HIV that Evolved Near-Pan Neutralization Breadth. Immunity *45*, 1108–1121.

Huang, Y., Yu, J., Lanzi, A., Yao, X., Andrews, C.D., Tsai, L., Gajjar, M.R., Sun, M., Seaman, M.S., Padte, N.N., and Ho, D.D. (2016b). Engineered Bispecific Antibodies with Exquisite HIV-1-Neutralizing Activity. Cell *165*, 1621–1631.

Igarashi, T., Brown, C., Azadegan, A., Haigwood, N., Dimitrov, D., Martin, M.A., and Shibata, R. (1999). Human immunodeficiency virus type 1 neutralizing antibodies accelerate clearance of cell-free virions from blood plasma. Nat. Med. *5*, 211–216.

Julg, B., Liu, P.T., Wagh, K., Fischer, W.M., Abbink, P., Mercado, N.B., Whitney, J.B., Nkolola, J.P., McMahan, K., Tartaglia, L.J., et al. (2017a). Protection against a mixed SHIV challenge by a broadly neutralizing antibody cocktail. Sci. Transl. Med. *9*, eaao4235.

Julg, B., Pegu, A., Abbink, P., Liu, J., Brinkman, A., Molloy, K., Mojta, S., Chandrashekar, A., Callow, K., Wang, K., et al. (2017b). Virological Control by the CD4-Binding Site Antibody N6 in Simian-Human Immunodeficiency Virus-Infected Rhesus Monkeys. J. Virol. *91*, e00498-17.

Khan, S.N., Sok, D., Tran, K., Movsesyan, A., Dubrovskaya, V., Burton, D.R., and Wyatt, R.T. (2018). Targeting the HIV-1 Spike and Coreceptor with Bi- and Trispecific Antibodies for Single-Component Broad Inhibition of Entry. J. Virol. *92*, e00384-18.

Klein, F., Halper-Stromberg, A., Horwitz, J.A., Gruell, H., Scheid, J.F., Bournazos, S., Mouquet, H., Spatz, L.A., Diskin, R., Abadir, A., et al. (2012). HIV therapy by a combination of broadly neutralizing antibodies in humanized mice. Nature *492*, 118–122.

Ko, S.Y., Pegu, A., Rudicell, R.S., Yang, Z.Y., Joyce, M.G., Chen, X., Wang, K., Bao, S., Kraemer, T.D., Rath, T., et al. (2014). Enhanced neonatal Fc receptor function improves protection against primate SHIV infection. Nature *514*, 642–645.

Ledgerwood, J.E., Coates, E.E., Yamshchikov, G., Saunders, J.G., Holman, L., Enama, M.E., DeZure, A., Lynch, R.M., Gordon, I., Plummer, S., et al.; VRC 602 Study Team (2015). Safety, pharmacokinetics and neutralization of the broadly neutralizing HIV-1 human monoclonal antibody VRC01 in healthy adults. Clin. Exp. Immunol. *182*, 289–301.

Li, M., Gao, F., Mascola, J.R., Stamatatos, L., Polonis, V.R., Koutsoukos, M., Voss, G., Goepfert, P., Gilbert, P., Greene, K.M., et al. (2005). Human immunodeficiency virus type 1 env clones from acute and early subtype B infections for standardized assessments of vaccine-elicited neutralizing antibodies. J. Virol. *79*, 10108–10125.

Liu, J., Ghneim, K., Sok, D., Bosche, W.J., Li, Y., Chipriano, E., Berkemeier, B., Oswald, K., Borducchi, E., Cabral, C., et al. (2016). Antibody-mediated

protection against SHIV challenge includes systemic clearance of distal virus. Science *353*, 1045–1049.

Liu, W., Wong, Y.C., Chen, S.M.Y., Tang, J., Wang, H., Cheung, A.K.L., and Chen, Z. (2018). DNA prime/MVTT boost regimen with HIV-1 mosaic Gag enhances the potency of antigen-specific immune responses. Vaccine *36*, 4621–4632.

Lu, X., Liu, L., Zhang, X., Lau, T.C.K., Tsui, S.K.W., Kang, Y., Zheng, P., Zheng, B., Liu, G., and Chen, Z. (2012). F18, a novel small-molecule nonnucleoside reverse transcriptase inhibitor, inhibits HIV-1 replication using distinct binding motifs as demonstrated by resistance selection and docking analysis. Antimicrob. Agents Chemother. *56*, 341–351.

Lu, C.L., Murakowski, D.K., Bournazos, S., Schoofs, T., Sarkar, D., Halper-Stromberg, A., Horwitz, J.A., Nogueira, L., Golijanin, J., Gazumyan, A., et al. (2016). Enhanced clearance of HIV-1-infected cells by broadly neutralizing antibodies against HIV-1 in vivo. Science *352*, 1001–1004.

Lynch, R.M., Boritz, E., Coates, E.E., DeZure, A., Madden, P., Costner, P., Enama, M.E., Plummer, S., Holman, L., Hendel, C.S., et al.; VRC 601 Study Team (2015). Virologic effects of broadly neutralizing antibody VRC01 administration during chronic HIV-1 infection. Sci. Transl. Med. *7*, 319ra206.

Mascola, J.R. (2002). Passive transfer studies to elucidate the role of antibody-mediated protection against HIV-1. Vaccine *20*, 1922–1925.

Mendoza, P., Gruell, H., Nogueira, L., Pai, J.A., Butler, A.L., Millard, K., Lehmann, C., Suárez, I., Oliveira, T.Y., Lorenzi, J.C.C., et al. (2018). Combination therapy with anti-HIV-1 antibodies maintains viral suppression. Nature *561*, 479–484.

Miller, C.J., Li, Q., Abel, K., Kim, E.Y., Ma, Z.M., Wietgrefe, S., La Franco-Scheuch, L., Compton, L., Duan, L., Shore, M.D., et al. (2005). Propagation and dissemination of infection after vaginal transmission of simian immunodeficiency virus. J. Virol. *79*, 9217–9227.

Moldt, B., Rakasz, E.G., Schultz, N., Chan-Hui, P.Y., Swiderek, K., Weisgrau, K.L., Piaskowski, S.M., Bergman, Z., Watkins, D.I., Poignard, P., and Burton, D.R. (2012). Highly potent HIV-specific antibody neutralization in vitro translates into effective protection against mucosal SHIV challenge in vivo. Proc. Natl. Acad. Sci. USA *109*, 18921–18925.

Montefiori, D.C. (2004). Evaluating Neutralizing Antibodies Against HIV, SIV, and SHIV in Luciferase Reporter Gene Assays. Curr. Protoc. Immunol. *64*, 12.11.1–12.11.17.

Nishimura, Y., Gautam, R., Chun, T.W., Sadjadpour, R., Foulds, K.E., Shingai, M., Klein, F., Gazumyan, A., Golijanin, J., Donaldson, M., et al. (2017). Early antibody therapy can induce long-lasting immunity to SHIV. Nature *543*, 559–563.

Pace, C.S., Song, R., Ochsenbauer, C., Andrews, C.D., Franco, D., Yu, J., Oren, D.A., Seaman, M.S., and Ho, D.D. (2013). Bispecific antibodies directed to CD4 domain 2 and HIV envelope exhibit exceptional breadth and picomolar potency against HIV-1. Proc. Natl. Acad. Sci. USA *110*, 13540–13545.

Parsons, M.S., Lee, W.S., Kristensen, A.B., Amarasena, T., Khoury, G., Wheatley, A.K., Reynaldi, A., Wines, B.D., Hogarth, P.M., Davenport, M.P., and Kent, S.J. (2019). Fc-dependent functions are redundant to efficacy of anti-HIV antibody PGT121 in macaques. J. Clin. Invest. *129*, 182–191.

Ryman, J.T., and Meibohm, B. (2017). Pharmacokinetics of Monoclonal Antibodies. CPT Pharmacometrics Syst. Pharmacol. *6*, 576–588.

Scheid, J.F., Horwitz, J.A., Bar-On, Y., Kreider, E.F., Lu, C.L., Lorenzi, J.C., Feldmann, A., Braunschweig, M., Nogueira, L., Oliveira, T., et al. (2016). HIV-1 antibody 3BNC117 suppresses viral rebound in humans during treatment interruption. Nature *535*, 556–560.

Schoofs, T., Klein, F., Braunschweig, M., Kreider, E.F., Feldmann, A., Nogueira, L., Oliveira, T., Lorenzi, J.C., Parrish, E.H., Learn, G.H., et al. (2016). HIV-1 therapy with monoclonal antibody 3BNC117 elicits host immune responses against HIV-1. Science *352*, 997–1001.

Seeds, R.E., Mukhopadhyay, S., Jones, I.M., Gordon, S., and Miller, J.L. (2011). The role of myeloid receptors on murine plasmacytoid dendritic cells in induction of type I interferon. Int. Immunopharmacol. *11*, 794–801.

Shingai, M., Nishimura, Y., Klein, F., Mouquet, H., Donau, O.K., Plishka, R., Buckler-White, A., Seaman, M., Piatak, M., Jr., Lifson, J.D., et al. (2013). Antibody-mediated immunotherapy of macaques chronically infected with SHIV suppresses viraemia. Nature *503*, 277–280.

Smith, K., Garman, L., Wrammert, J., Zheng, N.Y., Capra, J.D., Ahmed, R., and Wilson, P.C. (2009). Rapid generation of fully human monoclonal antibodies specific to a vaccinating antigen. Nat. Protoc. *4*, 372–384.

Steinhardt, J.J., Guenaga, J., Turner, H.L., McKee, K., Louder, M.K., O'Dell, S., Chiang, C.I., Lei, L., Galkin, A., Andrianov, A.K., et al. (2018). Rational design of a trispecific antibody targeting the HIV-1 Env with elevated anti-viral activity. Nat. Commun. *9*, 877.

Sun, C., Chen, Z., Tang, X., Zhang, Y., Feng, L., Du, Y., Xiao, L., Liu, L., Zhu, W., Chen, L., and Zhang, L. (2013). Mucosal priming with a replicating-vaccinia virus-based vaccine elicits protective immunity to simian immunodeficiency virus challenge in rhesus monkeys. J. Virol. *87*, 5669–5677.

Tiller, T., Meffre, E., Yurasov, S., Tsuiji, M., Nussenzweig, M.C., and Wardemann, H. (2008). Efficient generation of monoclonal antibodies from single human B cells by single cell RT-PCR and expression vector cloning. J. Immunol. Methods *329*, 112–124.

Walker, L.M., Huber, M., Doores, K.J., Falkowska, E., Pejchal, R., Julien, J.P., Wang, S.K., Ramos, A., Chan-Hui, P.Y., Moyle, M., et al.; Protocol G Principal Investigators (2011). Broad neutralization coverage of HIV by multiple highly potent antibodies. Nature *477*, 466–470.

Wen, Y.M., Mu, L., and Shi, Y. (2016). Immunoregulatory functions of immune complexes in vaccine and therapy. EMBO Mol. Med. *8*, 1120–1133.

Whitney, J.B., Hill, A.L., Sanisetty, S., Penaloza-MacMaster, P., Liu, J., Shetty, M., Parenteau, L., Cabral, C., Shields, J., Blackmore, S., et al. (2014). Rapid seeding of the viral reservoir prior to SIV viraemia in rhesus monkeys. Nature *512*, 74–77.

Wiseman, R.W., Karl, J.A., Bohn, P.S., Nimityongskul, F.A., Starrett, G.J., and O'Connor, D.H. (2013). Haplessly hoping: macaque major histocompatibility complex made easy. ILAR J. *54*, 196–210.

Wu, X., Yang, Z.Y., Li, Y., Hogerkorp, C.M., Schief, W.R., Seaman, M.S., Zhou, T., Schmidt, S.D., Wu, L., Xu, L., et al. (2010). Rational design of envelope identifies broadly neutralizing human monoclonal antibodies to HIV-1. Science *329*, 856–861.

Wu, X., Guo, J., Niu, M., An, M., Liu, L., Wang, H., Jin, X., Zhang, Q., Lam, K.S., Wu, T., et al. (2018). Tandem bispecific neutralizing antibody eliminates HIV-1 infection in humanized mice. J. Clin. Invest. *128*, 2239–2251.

Xu, L., Pegu, A., Rao, E., Doria-Rose, N., Beninga, J., McKee, K., Lord, D.M., Wei, R.R., Deng, G., Louder, M., et al. (2017). Trispecific broadly neutralizing HIV antibodies mediate potent SHIV protection in macaques. Science *358*, 85–90.

Yamamoto, T., Lynch, R.M., Gautam, R., Matus-Nicodemos, R., Schmidt, S.D., Boswell, K.L., Darko, S., Wong, P., Sheng, Z., Petrovas, C., et al. (2015). Quality and quantity of TFH cells are critical for broad antibody development in SHIVAD8 infection. Sci. Transl. Med. *7*, 298ra120.

Zhao, L., Ji, P., Li, Z., Roy, P., and Sahajwalla, C.G. (2013). The antibody drug absorption following subcutaneous or intramuscular administration and its mathematical description by coupling physiologically based absorption process with the conventional compartment pharmacokinetic model. J. Clin. Pharmacol. *53*, 314–325.

Zhou, T., Zheng, A., Baxa, U., Chuang, G.Y., Georgiev, I.S., Kong, R., O'Dell, S., Shahzad-Ul-Hussan, S., Shen, C.H., Tsybovsky, Y., et al.; NISC Comparative Sequencing Program (2018). A Neutralizing Antibody Recognizing Primarily N-Linked Glycan Targets the Silent Face of the HIV Envelope. Immunity *48*, 500–513.e6.

STAR★METHODS

KEY RESOURCES TABLE

REAGENT or RESOURCE	SOURCE	IDENTIFIER
Antibodies		
BilA-SG produced from Chinese hamster ovary cells	This paper	N/A
Human IgG for isotype control for *in vivo* half-life study using CMRs	Guizhou Taibang Biological Products	N/A
Anti-CD8β mAb CD8b255R1 for *in vivo* CD8 depletion	National Institutes of Health Nonhuman Primate Reagent Resource Program	Cat# AB_271632; RRID: AB_2716321
Horseradish peroxidase-conjugated goat anti-human IgG antibody for ELISA	Invitrogen	Cat# 62-8420; RRID: AB_2533962
Horseradish peroxidase-conjugated anti-monkey immunoglobulin G antibody for ELISA	Southern Biotech	Cat# 4700-05; RRID: AB_2796069
Anti-CD28 (CD28.2) for activation	BioLegend	Cat# 302934; RRID: AB_11148949
Anti-CD49d (9F10) for activation	BioLegend	Cat# 304301, RRID; AB_314427
Anti-CD3 (SP34-2; Horizon V450)	BD Biosciences	Cat# 560351; RRID: AB_1645168
Anti-CD4 (OKT4; PerCP-Cy5.5)	BioLegend	Cat# 317427; RRID: AB_1186124
Anti-CD8α (RPA-T8; APC)	BioLegend	Cat# 300912; RRID: AB_314116
Anti-IFN-γ (B27; PE)	BioLegend	Cat# 506506; RRID: AB_315439
Anti-TNFα (Mab11; FITC)	BioLegend	Cat# 502906; RRID: AB_315258
Anti-IL-2 (MQ1-17H12; PE-Cy7)	BD Biosciences	Cat# 560707; RRID: AB_1727542
Bacterial and virus strains		
$SHIV_{SF162P3}$	Prof. Cecilia Cheng-Mayer (ADARC, Rockefeller University)	N/A
$SHIV_{SF162P3CN}$	This paper	N/A
Biological samples		
$SHIV_{SF162P3CN}$ infected or uninfected macaque PBMCs	This paper	N/A
Chemicals, peptides, and recombinant proteins		
HIV-1_{JRFL} gp120 for BilA-SG ELISA	SinoBiological	Cat# 40404-V08H
HIV-1_{SF162} gp120 for endogenous antibody ELISA	NIH AIDS Reagents Program	Cat# ARP-12026
SIV_{mac239}-p27 for endogenous antibody ELISA	In-house	N/A
SIVmac239 Gag-p57 peptide array	NIH AIDS Reagents Program	Cat# 6204
SIVmac239 Nef peptide array	NIH AIDS Reagents Program	Cat# 8762
SIVmac239 Env peptide array (HIV consensus B)	NIH AIDS Reagents Program	Cat# ARP-9480
Cell Activation Cocktail (without Brefeldin A)	BioLegend	Cat# 423302
Brefeldin A	Sigma-Aldrich	Cat# B6542-25MG
Cytofix/Cytoperm Fixation/ Permeabilization Kit	BD Biosciences	Cat# 554714; RRID: AB_2869008
Zombie Aqua fixable viability stain	BioLegend	Cat# 77143
Critical commercial assays		
QIAamp Viral RNA Minikit	QIAGEN	Cat# 52904
QIAamp DNA Mini Kit	QIAGEN	Cat# 51304
PrimeScript 1st strand cDNA synthesis kit	Takara	Cat# 6110A

(*Continued on next page*)

Continued

REAGENT or RESOURCE	SOURCE	IDENTIFIER
Superscript IV Reverse Transcriptase	Invitrogen	Cat# 18090010
TB Green Premix Ex TaqII	Takara	Cat# RR820A
QuantStudio 3D Digital PCR Master Mix v2	Applied Biosystem	Cat# A26358
Q5 High-Fidelity DNA Polymerase	BioLabs	Cat# M0491L
Monkey IFN-γ T cell ELISPOT kit	Mabtech	Cat# 3421M-2A
Nano-Glo® Luciferase Assay System	Promega	Cat# N1130
Non-human primate $CD8^+$ T cell Isolation Kit (for $CD8^+$ T cell depletion in SHIV stock generation)	Miltenyi Biotech	Cat# 130-092-143
Experimental models: Cell lines		
TZM-bl	NIH HIV Reagent Program	Cat# 8129-442; RRID: CVCL_B478
Experimental models: Organisms/strains		
Rhesus macaques (M.mulatta) of Chinese genetic origin	Foshan University	N/A
Oligonucleotides		
SIV-Gag-specific primers for plasma viral load: Forward: 5′-GTAGTATGGGCAGCA AATGAAT-3′ Reverse: 5′- CACCAG ATGACGCAGACAGTAT-3′	Lu et al., 2012	N/A
SIV-Gag specific primers for proviral: Forward: 5′-GTCTGCGTCATYTGGT GCATTC-3′ Reverse: 5′-CACTAGY TGTCTCTGCACTATRTGTTTTG-3′, Probe: 5′-FAM-CTTCRTCAGTYTG TTTCACTTTCTCTTC-TGCG-BHQ1-3′	Cline et al., 2005	N/A
SHIV SGA reverse transcription primer: SHIV SGA EnvR1: 5′-CAATAATTGTCT GGCCTGTACCGTC-3′	Julg et al., 2017a	N/A
SHIV SGA nested PCR 1st round primer: Forward (SHIV SGA EnvF1): 5′-TATGGGG TACCTGTGTGGAA-3′ Reverse: SHIV SGA EnvR1	Julg et al., 2017a	N/A
SHIV SGA nested PCR 2nd round primer: Forward (SHIV SGA EnvF2): 5′-GCCTG TGTACCCACAGAC-3′ Reverse (EnvR2): 5′-ATAGTGCTTCCTGCTGC-3′	Julg et al., 2017a	N/A
Software and algorithms		
FlowJo v9.9	BD Biosciences	RRID: SCR_008520
Prism v7	GraphPad	RRID: SCR_002798
Other		
QuantStudio 3D Digital PCR system	Applied Biosystem	Cat# 44-890-84
FACSAria III	BD Biosciences	RRID: SCR_016695

RESOURCE AVAILABILITY

Lead contact

Further information and requests for resources and reagents should be directed to and will be fulfilled by the lead contact, Zhiwei Chen (zchenai@hku.hk).

Materials availability

All resources and reagents used in this study are available upon request from the lead contact.

Data and code availability

- The data that support the findings of this study are available upon request from the lead contact.
- This paper does not report original code.
- Any additional information required to reanalyze the data reported in this paper is available from the lead contact upon request.

EXPERIMENTAL MODEL AND SUBJECT DETAILS

Animals and study design

The overall objective of this study was to investigate the prophylactic and therapeutic efficacy of BiIA-SG against the high-dose of $SHIV_{SF162P3CN}$ challenge. 35 3 year-old female rhesus macaques (*M.mulatta*) of Chinese genetic origin were housed and cared in the Department of Veterinary Medicine at the Foshan University. Four sub-studies were performed including (1) to determine the pharmacokinetics study of BiIA-SG in CRMs, (2) to characterize infectivity and pathogenicity of $SHIV_{SF162P3CN}$ challenge stock by high-dose intravenous challenge in CRMs, (3) to test the prophylactic efficacy and (4) to test the therapeutic activity of BiIA-SG in acute $SHIVS_{F162P3CN}$-infected macaques. All of the macaques used in this study were genotyped as previously described (Wiseman et al., 2013). Major histocompatibility complex class I (MHC-I) class I and tripartite motif-containing protein 5 (TRIM5) polymorphisms were balanced equally among groups/were randomly allocated in each group. Blood was collected regularly to monitor viral infection, passively transferred monoclonal antibody concentrations and serum neutralizing activity. For the half-life study, 4 naive CRMs were injected 10mg/kg BiIA-SG intramuscularly, whereas 4 control CMRs were injected the same dose of human IgG (Guizhou Taibang Biological Products). The rest of 27 CRMs were all inoculated with $5000TCID_{50}$ $SHIV_{SF162P3CN}$ intravenously. The inoculum of 5000 $TCID_{50}$ contains about $2.5x10^6$ copies/ml of viral RNA. Eight untreated CRMs received saline and were used as control for the pathogenesis study. For the prophylactic study, 3 CRMs were intramuscularly and 3 CRMs were intravenously infused with 10mg/kg BiIA-SG 24 hours before viral challenge. For the therapeutic study, 7 CRMs were treated with 20mg/kg BiIA-SG intramuscularly 24 hours post-infection, whereas 6 CRMs were treated with the same dose of BiIA-SG 72 hours post-infection.

Study approval

All animal studies were performed in accordance with protocols approved by the Institutional Animal Care and Use Committee of the Department of Veterinary Medicine at the Foshan University.

METHOD DETAILS

Preparation of $SHIV_{SF162P3CN}$ challenge stock

Our parental R5-tropic $SHIV_{SF162P3}$ strain was a gift from Prof. Cecilia Cheng-Mayer. This strain was isolated from a R5-tropic $SHIV_{SF162P3}$-infected Indian rhesus macaque DV60 at the end stage of simian AIDS (Harouse et al., 2001). Accordingly, this strain maintained its CCR5-tropism. The $SHIV_{SF162P3CN}$ challenge stock was then generated by expansion in IL-2-treated Chinese (CN) rhesus macaque PBMCs that were depleted of $CD8^+$ T cells by magnetic bead separation (Miltenyi Biotech). $TCID_{50}$ of the $SHIV_{SF162P3CN}$ stock was determined by TZM-bl cells based luciferase reporter assays (Montefiori, 2004). Amino acid sequence alignment of HIV-1_{SF162}, $SHIV_{SF162P3}$ and challenge stock $SHIV_{SF162P3CN}$ gp120 and mutations generated in challenge stock during preparation (B) are shown in Figure S6.

Antibodies

BiIA-SG was produced by contract manufacture by GLP-grade manufacturing company from Chines hamster ovry cells standard as previously described (Wu et al., 2018) and purified by chromatography and sterile filtration and were endotoxin-free. Plasma BiIA-SG antibody concentration was measured by enzyme-linked immunosorbent assays (ELISA) (Walker et al., 2011). HIV-1_{JRFL} gp120 was used as a capture protein for BiIA-SG. Bound antibodies were detected horseradish peroxidase-conjugated goat anti-human IgG antibody (Santa Cruz Biotechnology).

Viral quantitation assays

Viral RNA isolated from monkey plasma using a QIAamp Viral RNA Minikit (QIAGEN) was reversed transcribed into viral complementary DNA (cDNA) using a PrimeScript 1^{st} strand cDNA synthesis kit (Takara) with random hexamers. Plasma viral RNA copy number was determined by real-time quantitative PCR (qPCR) with a SYBR green premix Ex Taq (Takara) and SIV-Gag-specific primers 5′-GTAGTATGGGCAGCAAATGAAT-3′ and 5′- CACCAGATGACGCAGACAGTAT-3′ (Lu et al., 2012). The limit of detection is 200 copies/ml for this viral load determination. To determine cell-associated DNA viral load, DNA was first isolated from PBMCs using a QIAamp DNA Mini Kit (QIAGEN). Digital PCR was then performed on the QuantStudio 3D Digital PCR system (Thermo Fisher) to determine proviral loads, with primers 5′-GTCTGCGTCATYTGGTGCATTC-3′ and 5′-CACTAGYTGTCTCTGCACTATRTGTTTTG-3′, and probe 5′-FAM-CTTCRTCAGTYTGTTTCACTTTCTCTTCTGCG-BHQ1-3′ (Cline et al., 2005). The results were normalized

with cell numbers calculated based on albumin gene copy numbers determined by real-time quantitative PCR (Chung et al., 2008). Accordingly, the limit of digital PCR detects single copy of proviral DNA.

Humoral response

Detection of endogenous antibodies titers was performed by ELISA as previously described (Gautam et al., 2018; Wu et al., 2018). In brief, high-binding 96-well plates were coated with 50ng BilA-SG, SIV_{mac239}-p27 or HIV-1 $_{SF162}$ gp120 protein overnight at 4°C and blocked at 37°C for 2 hours. Heat inactivated serum were fivefold serial diluted in blocking buffer and were added to plates for incubating 1h at 37°C, followed by 3 times of PBS-0.05%Tween washing. Bound antibodies were detected by using a horseradish peroxidase-conjugated anti-monkey (SouthernBiotech) immunoglobulin G antibody with minimal cross-reactivity to human mAb. Blank wells containing assay diluent of each plate were used as background. Fivefold of blank wells mean optical density (OD) were used as a cutoff. The log values of these antibodies were reported as the endpoint dilution of endogenous antibodies titers.

Cellular immune assays

T cell immune responses were examined by IFN-γ ELISpot or intracellular cytokine staining (ICS) assays. In ELISpot assays, PBMC responses were measured by *in vitro* 1 μg/ml of 15-mer overlapping peptide pools spanning the full-length SIVmac239 Gag-p57 antigens, Nef, Env (HIV consensus B) (NIH AIDS Reagents Program), and the T cell responses were determined using monkey IFN-γ T cell ELISPOT kit (Mabtech) as previously described (Liu et al., 2018; Sun et al., 2013). In ICS assays, up to $1x10^6$ PBMCs were stimulated with 1 μg/ml of 15-mer overlapping Gag-p57 or Nef peptide pools in the presence of 0.5 μg/ml of anti-CD28 (CD28.2) and anti-CD49d (9F10) antibodies (Biolegend). Backgrounds were determined in co-stimulated cells without the presence of antigens. Phorbol-12-myristate 13-acetate (81nM) and ionomycin (1.3μM) were used as positive control stimulant (Biolegend). After 2-hour incubation at 37°C with 5% CO_2, Brefeldin A (7.5 μg/ml; Sigma-Aldrich) was added, and the cells were further incubation overnight. Cells were then surface stained, fixed and permeabilised using Cytofix/Cytoperm kit (BD Biosciences), and stained for intracellular cytokines. The following antibodies were used: anti-CD3 (SP34-2; Horizon V450), anti-CD4 (OKT4; PerCP-Cy5.5), anti-CD8α (RPA-T8; APC), anti-IFN-γ (B27; PE), anti-TNFα (Mab11; FITC), anti-IL-2 (MQ1-17H12; PE-Cy7). The antibodies were from BD Biosciences or Biolegend. Zombie Aqua fixable viability stain was used during the surface staining step to discriminate against dead cells. Data were acquired with a BD FACSAria III instrument and analyzed using FlowJo v9.9 software.

Neutralization antibody assay

In vitro neutralization activity of bNAbs or bi-bNAbs was measured against the $SHIV_{SF162P3CN}$ challenge strain by a standard protocol using TZM-bl target cells and a luciferase reporter assay as previously described (Li et al., 2005). The antibodies tested were first pre-incubated with an inoculum of 200 $TCID_{50}$ $SHIV_{SF162P3CN}$, followed by addition of TZM-bl target cells. Infection was measured by the luciferase assay 48 hours later. The 50% inhibitory dilution (ID_{50}) or 80% inhibitory dilution (ID_{80}) of monkey serum was calculated to reflect antiviral potency.

$CD8^+$ T cell depletion *in vivo*

Four out of eight controller macaques were intravenously injected with a single dose (50mg/kg) of anti-CD8β mAb CD8b255R1 (National Institutes of Health Nonhuman Primate Reagent Resource Program).

Single-genome amplification (SGA)

SGA followed by direct sequencing of the Env gene was performed as previously described (Julg et al., 2017a). In brief, viral RNA was isolated from monkey plasma by QIAamp viral RNA kit (QIAGEN) and reverse transcribed to cDNA by using Superscript IV Reverse Transcriptase (Invitrogen) with gene-specific primer, SHIV SGA EnvR1 (5′-CAATAATTGTCTGGCCTGTACCGTC-3′). The cDNA templates were serially diluted until less 30% amplicons are positive after the two-round nested PCR. The first-round PCR was conducted by using Q5 High-Fidelity DNA Polymerase along with SHIV SGA EnvF1 (5′-TATGGGGTACCTGTGTGGAA-3′) and SHIV SGA EnvR1. After that, the first-round PCR product was diluted for 100 times and only use 1 microliter as template for the second-round PCR with primers SHIV SGA EnvF2 (5′-GCCTGTGTACCCACAGAC-3′) and EnvR2 (5′-ATAGTGCTTCCTGCTGC-3′). For each sample, around 25-35 amplicons were sequenced and analyzed.

QUANTIFICATION AND STATISTICAL ANALYSIS

Statistical analyses of data were performed using Prism v7 (GraphPad).Two-tailed Wilcoxon rank sum test or Kruskal-Wallis test followed by the Dunn's multiple comparisons test were performed for the comparisons between two treatment groups or more than two treatment groups, respectively. Survival analysis was performed using the log-rank test. Probability value (p) of smaller than 0.05 was considered statistically significant.